ADVANCED SUSTAINABLE SYSTEMS
www.advsustainsys.com

The Global Warming Potential of Geoengineering via Radiative Cooling

*Atousa Pirvaram, Siu Ning Leung, and Paul G. O'Brien**

This paper analyzes the potential to mitigate global warming using radiative cooling (RC) surfaces on a large scale. The study evaluates the net cooling power, radiative forcing (RF), and global warming potential of different RC materials compared to conventional construction and roofing materials, Earth's natural surfaces, and some reference cases. Key parameters for evaluating the above-mentioned structures include their solar reflectance (albedo) and long-wavelength infrared emissivity. Results show the cooling power that can be achieved by an ideal RC material with a solar reflectance of 100% and long-wave infrared emissivity of 100% is 164.8 W·m^{-2}. In practice, materials exhibiting a cooling power as high as 160.8 W·m^{-2} are fabricated. Further analysis shows if 1% of Earth's surface are to be covered with this material the terrestrial RF will decrease by 1.61 W·m^{-2} (from 0.6 to −1.01 W·m^{-2}). The results demonstrate that RC materials with high solar reflectivity and emissivity offer substantial cooling benefits and can reduce RF when implemented on large scales. The findings underscore the effectiveness of RC materials in reducing global warming and provide a valuable perspective on their role in reducing the environmental impacts of the built environment.

1. Introduction

According to the International Panel on Climate Change, global warming due to human activities has caused Earth's temperature to increase by ≈1 °C as compared to pre-industrial levels. If the current rate of increase continues, Earth's temperature will likely surge by 1.5 °C between 2030 and 2050 due to global warming.[1] The Earth's temperature is influenced by a complex exchange of radiant energy, wherein the atmosphere and surface absorb incoming solar radiation and emit thermal radiation in the infrared spectrum to outer space. The increasing severity of climate change has brought the concept of radiative forcing (RF) to the forefront of environmental science. Changes in RF, which is a measure of the imbalance of radiative heat transfer between the Earth's atmosphere and outer space, has been a critical indicator of how human activities are driving global warming. According to recent scientific reports, the rise in RF is directly linked to significant alterations in the Earth's climate, leading to rising sea levels, more frequent extreme weather events, and ecosystem disruptions. RF, measured in W·m^{-2}, represents the difference between the incoming and outgoing radiant energy between Earth's atmosphere and outer space.[2] RF increases when atmospheric greenhouse gases absorb outgoing radiation, leading to higher climatic temperatures.[3,4]

The Paris Agreement, which came into effect in 2016, is a legally obligatory international agreement to reduce emissions and combat climate change. Its main objective is to limit global temperature increases to much lower than 2 °C above pre-industrial levels, while pursuing efforts to limit the increase to 1.5 °C. The agreement encompasses various measures including cutting global greenhouse gas emissions, promoting adaptation, and enhancing transparency and support mechanisms for climate action.[5] Emissions reductions and removing carbon dioxide from the atmosphere, collectively referred to as "mitigation," along with reducing damage by adapting to climate risks and impacts, are recognized strategies for combating global warming and its effects. Climate change mitigation strategies can be broadly categorized into two approaches: emission reduction and geoengineering. Emission reduction focuses on minimizing the release of greenhouse gases, primarily through renewable energy adoption, energy efficiency improvements, and reforestation efforts. These methods address the root cause of global warming by reducing the atmospheric concentration of greenhouse gases. Conventional decarbonization strategies include fuel switching, efficiency improvements, and nuclear power. On the other hand, geoengineering strategies involve intentionally altering Earth's climate system to counteract global warming. In geoengineering approaches such as Solar Radiation Management (SRM), which is also known as solar engineering, a portion of the Sun's energy is reflected into space. Techniques in this category used to manage RF include stratospheric aerosol injection, marine cloud brightening, cir-

A. Pirvaram, S. N. Leung, P. G. O'Brien
Department of Mechanical Engineering
Lassonde School of Engineering
York University
Toronto, OntarioM3J 1P3, Canada
E-mail: paul.obrien@lassonde.yorku.ca

The ORCID identification number(s) for the author(s) of this article can be found under https://doi.org/10.1002/adsu.202400948

DOI: 10.1002/adsu.202400948

rus cloud thinning, space-based mirrors, surface-based brightening, and various other radiation management strategies.[6–9] Despite the help of SRM in mitigating the climate risk and minimizing ecosystem degradation, it does not tackle the underlying causes of global warming, nor does it fully reverse all the climate changes induced by greenhouse gases. This means that if SRM efforts were to cease, temperatures could rapidly rebound, potentially causing more harm[7] Carbon Dioxide Removal (CDR) is another geoengineering strategy that refers to any practice that includes removing and restoring CO_2. It is proposed for CO_2 to be captured directly from the atmosphere using negative emissions technologies or CO_2 removal methods. These methods include bioenergy with carbon capture and storage, biochar production, enhanced weathering, direct air capture, ocean fertilization, ocean alkalinity enhancement, soil carbon sequestration, afforestation and reforestation, wetland restoration, mineral carbonation, and using biomass in construction.[8,9] However, while CDR technologies like direct air capture are theoretically scalable, the infrastructure required to remove significant amount of CO_2 from the atmosphere is immense and costly. Current CDR methods are expensive and scaling them to the necessary level may not be economically feasible in the short term. Similar to SRM, there is a concern that the prospect of CDR could lead to complacency in reducing emissions. Policymakers and industries might rely too heavily on the future success of CDR technologies instead of immediately reducing emissions. Therefore, despite these mitigation efforts, global warming due to increasing RF levels remains a significant and pressing challenge. Furthermore, global warming rates are expected to increase as global energy consumption and emissions continue to rise. For example, the International Energy Agency predicts a three-fold increase in the global energy demand for air conditioning by 2050, which could accelerate global warming due to the abundant amount of greenhouse gases emitted by these systems.[10–13]

In recent years, radiative cooling (RC) has emerged as a promising geoengineering approach. Unlike SRM and CDR, RC leverages the natural ability to emit infrared radiation into outer space, passively cooling surfaces without additional energy input. Advanced materials designed for RC can reflect solar radiation while efficiently emitting thermal radiation, potentially mitigating the warming effects associated with RF. That is, RC technology cools terrestrial objects by emitting radiation to outer space over a spectral region where the atmosphere is highly transparent (from ≈8 to 13 μm). This process can be implemented on a large scale as a geoengineering method to alleviate global warming while reducing energy consumption and emissions associated with cooling loads.[14–20] Recent advancements in RC technology focus on elevating the cooling power of novel materials and structural designs by increasing the solar reflectance and long-wave infrared emissivity.[21–24] For instance, the study conducted by Liu et al.[25] introduces innovative approaches, including hierarchical micro/nanostructures and doped polymer-based films, which enhance spectral selectivity and durability for real-world applications. In studies reported by Pirvaram et al.[26] and Chiu et al.,[27] the effects of placing underside reflectors on the cooling performance of RC materials are investigated. Pirvaram et al.[26] show that employing reflectors significantly increase the cooling power of the RCs while achieving temperature well below the ambient. In particular, a parabolic reflective dish decreases the steady state temperature a selective RC can potentially achieve to temperatures as low as 229 in a 300 K ambient. The study conducted by Chiu et al.[27] demonstrates that placing a parabolic trough with a focal length of 0.016 m, a height of 0.635 m, and a length of 1 m results in sub-ambient cooling temperatures of 273.5 and 232.7 K when the RC is a broadband and selective emitter, respectively. Integrating these advancements into RC surfaces can significantly improve their effectiveness in mitigating urban heat and reducing energy consumption, making them viable for large-scale deployment. Guo et al.[28] also presents current challenges and future development trends of RC.

RC technology addresses global warming through two key mechanisms: 1) as a passive cooling method, it conserves electricity by lowering the cooling load in buildings, which indirectly reduces CO_2 emissions from electricity production; and 2) by enhancing the radiative heat flow from Earth to outer space, thereby decreasing RF and potentially achieving negative RF.[19] Despite its potential, the environmental implications and life cycle assessment (LCA) of RC have not been thoroughly investigated.

This paper presents LCA methods for determining the impact of using RC materials in place of other surfaces on the global warming potential (GWP) when the enhancement of RCs on increasing the radiative heat flow from Earth to outer space is considered. Specifically, the GWP associated with RC materials reported by Pirvaram et al.,[29] Wang et al.,[30] and Li et al., [31] are compared to the GWP associated with common construction materials such as white cement paste, road asphalt, concrete, and grey cement. Also, the GWP for common roofing materials including shingles, ceramic roofing tiles, and PVC roofing materials, as well as natural surfaces like forests and oceans, are analyzed. To further contextualize our results, the GWP for idealized surfaces such as a perfect RC, a perfect reflector, and a blackbody are considered. This study investigates the impact of covering 1% of the Earth's surface on the terrestrial RF and the resulting change in RF. The results contribute to a deeper understanding of how surface modifications may influence RF, thereby informing discussions surrounding climate mitigation strategies and land use planning. This study directly supports the United Nations Sustainable Development Goals (SDGs), particularly Goal 7: Affordable and Clean Energy, Goal 9: Industry, Innovation, and Infrastructure, and Goal 13: Climate Action. By analyzing the potential of RC materials to mitigate global warming on a large scale, this research offers an innovative and sustainable solution to reduce energy demands and greenhouse gas emissions associated with cooling systems. The demonstrated decrease in terrestrial RF when RC materials are employed highlights their capacity to address climate change (SDG 13) while promoting energy-efficient infrastructure (SDG 7 and SDG 9). Furthermore, the findings emphasize the critical role of advanced materials in creating sustainable urban environments and reducing the environmental impacts of the built environment, aligning with the broader objectives of the SDGs.

2. Methods

2.1. Determining the Net Cooling Power and Radiative Forcing

The net cooling power, $P_{\text{net cooling}}$, is a critical metric for evaluating the performance of RC materials and systems. It is determined

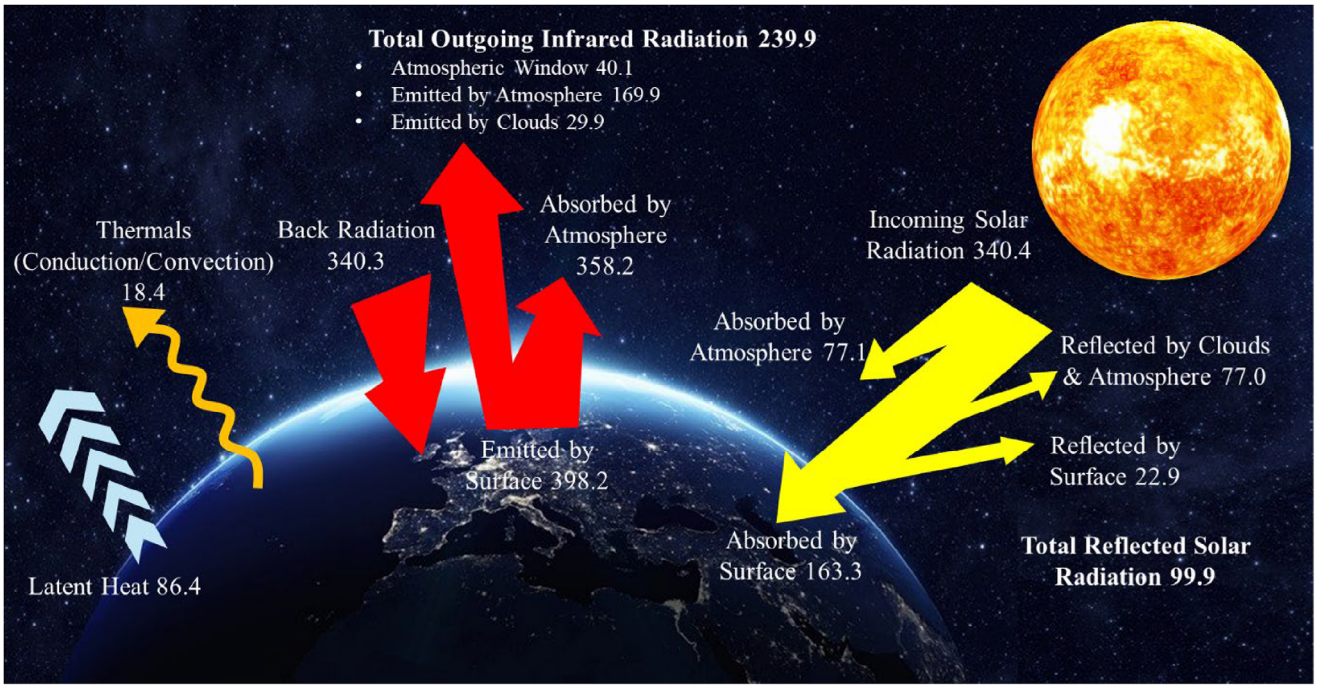

Figure 1. Global energy balance. Numerical values indicate the magnitudes of individual energy fluxes, measured in W·m^{-2} as reported by NASA.[32,33]

by the balance between the cooling power provided by thermal radiation and the heat gains from solar absorption, convection, and conduction. The net cooling power is calculated using Equation 1:[26]

$$P_{\text{net, Cooling}}\left(T_{\text{RC}}\right) = P_{\text{RC}}\left(T_{\text{RC}}\right) - P_{\text{atm}}\left(T_{\text{amb}}\right) - P_{\text{Solar}} - P_{\text{Conv.}}\left(T_{\text{RC}}, T_{\text{amb}}\right) \quad (1)$$

where P_{RC} is the radiative heat transfer from RC to outer space, P_{atm} is the atmospheric downward thermal radiation received by the RC, P_{solar} is the solar irradiance absorbed by the RC, and $P_{\text{Conv.}}$ is the convective heat transferred from the surroundings, respectively. Furthermore, T_{RC} and T_{amb} are the RC sample and ambient temperatures, respectively. $P_{\text{net cooling}}$ represents the intrinsic cooling capacity of an RC material, measured as the net power emitted per unit area of the material (W·m^{-2}) and is a material-specific property that quantifies the ability of an RC material to emit long-wavelength infrared radiation while reflecting incoming solar and atmospheric radiation incident on it. This term is widely used in the RC field to evaluate and compare the performance of developed RC materials on the earth's surface.

RF, also measured in W·m^{-2}, refers to the difference between the among of radiant energy entering and exiting Earth's atmosphere (measured at the top of the atmosphere). This study quantifies the changes in the balance between incoming solar radiation and outgoing terrestrial radiation due to the properties of different materials. By emitting heat directly into space, RC materials can induce a negative RF, helping to counteract the warming effects of greenhouse gases. A schematic diagram utilizing data reported by NASA depicting the global mean energy balance of the Earth is presented in **Figure 1**. The radiative heat transfer values presented in Figure 1 are used in conjunction with Equation 1 to examine how the surface albedo and emissivity of different materials influence the energy balance between the Earth and outer space.[32,33] The numerical values in Figure 1 denote the best estimates of the globally averaged incoming and outgoing radiant energy. As shown in Figure 1, the average incident solar irradiance per square meter at the top of the atmosphere (TOA) is ≈340.4 W, with 186.2 W·m^{-2} reaching the Earth's surface, $P_{\text{SolarToEarth}}$. Out of the solar irradiance reaching Earth's surface 163.3 W·m^{-2} is absorbed while 22.9 W·m^{-2} is reflected into space. The solar irradiance absorbed by Earth's surface is converted into heat energy. The Earth's surface emits longer wavelength infrared radiation. As a rough approximation, an average emissivity for Earth's surface, $\bar{\varepsilon}_{\text{Earth}}$, is ≈95%, owing to the prevalence of natural land and water surfaces with relatively high emissivity values. This results in a thermal outgoing flux at the TOA of ≈239.9 W·m^{-2}. Accordingly, there is an imbalance of 0.6 W·m^{-2} in the incoming and outgoing radiation at the TOA causing the Earth's temperature to increase. Notably, in comparison, Johnson et. al. have estimated the imbalance of the RF to be 0.71 W·m^{-2}.[34]

The optical properties of materials at the Earth's surface affect its radiative energy balance with outer space. The effects of different surfaces on the RF can be determined considering Equations 2 and 3. RF is the difference between the total incoming power (solar radiation) absorbed by the Earth and the total outgoing thermal radiation emitted by the Earth back into space at the TOA. The equation for calculating RF is given by:

$$RF = \sum P_{\text{Incoming, TOA}} - \sum P_{\text{Outgoing, TOA}} = P_{\text{Solar}-} P_{\text{ReflectedSolar}-} P_{\text{TotalEmitted}} \quad (2)$$

where $P_{\text{Incoming, TOA}}$ is the incoming thermal radiation at the TOA, $P_{\text{Outgoing, TOA}}$ is the outgoing thermal radiation emitted by the Earth at the TOA, P_{Solar} is the total incoming solar radiation, $P_{\text{ReflectedSolar}}$ is the total reflected solar radiation by the atmosphere and Earth's surface, and $P_{\text{TotalEmitted}}$ is the total radiation emitted by the atmosphere and the Earth's surface. As shown in Figure 1, the average incoming solar radiation at the TOA is 340.4 W·m^{-2}, the total outgoing radiation at the TOA is 239.9 W·m^{-2} (and the imbalance is 0.6 W·m^{-2}).

The RF that would occur if different materials were placed on top of the Earth's surface can be estimated by incorporating the average surface albedo ($\bar{R}_{\text{solar}}$) and the average long wavelength infrared emissivity ($\bar{\varepsilon}_{\text{LWIR}}$) into the balance for RF, as shown in Equation 3:

$$RF_i = P_{\text{Solar}} - \left(\bar{R}_{\text{solar}} \times P_{\text{SolarToEarth}}\right) - \left(P_{\text{ReflectedSolar\_atm}}\right) - \left(\left(\frac{\bar{\varepsilon}_{\text{LWIR}}}{\bar{\varepsilon}_{\text{Earth}}}\right) \times P_{\text{Emitted\_AW}} + P_{\text{Emitted\_atm}} + P_{\text{Emitted\_Clouds}}\right) \quad (3)$$

where $P_{\text{Emitted\_AW}}$, $P_{\text{Emitted\_Atm}}$, and $P_{\text{Emitted\_Clouds}}$ are the thermal radiation emitted by Earth's surface and passing through the atmospheric window (40.1 W·m^{-2}), emitted by the atmosphere (169.9 W·m^{-2}), and emitted by the clouds (29.9 W·m^{-2}), respectively.

2.2. Determining the Global Warming Potential Using the Net Cooling Power of Different Materials

The GWP compares the impact of the emissions of a particular gas on RF to that of CO_2 over a specific time horizon. The GWP for an emitted substance, i, can be calculated using Equation 4:[3]

$$GWP_i(H) = \frac{AGWP_i(H)}{AGWP_{CO_2}(H)} = \frac{\int_0^H RF_i(t)\,dt}{\int_0^H RF_{CO_2}(t)\,dt} \quad (4)$$

where $AGWP_i(H)$ and $AGWP_{CO_2}(H)$ are the absolute GWPs for substance i, and for CO_2, respectively. In essence, the GWP of a substance is determined by comparing the time-integrated global RF caused by a pulse emission of that substance to that of an equivalent mass of CO_2 over the specified time horizon of H. GWP is measured in carbon dioxide equivalents (CO_{2eq}) and varies with the time horizon because different substances decay at different rates in the atmosphere. For instance, methane (CH_4) has a GWP of 84–87 $kgCO_{2\text{-eq}}$ over a 20-year horizon and 28–36 $kgCO_{2\text{-eq}}$ over a 100-year horizon.[35]

The absolute GWP for a substance, assuming its removal from the atmosphere follows exponential decay, can be determined using Equation 5:

$$AGWP_i(H) = A_i\tau_i\left(1 - \exp\left(-\frac{H}{\tau_i}\right)\right) \quad (5)$$

where A_i is the radiative efficiency (RE) and τ_i is the lifetime of substance i in the atmosphere. The expression for $AGWP\,CO_{2\text{-eq}}$ is more complicated due to the absorption and transport processes in the ocean over different timescales. The decomposition of CO_2 in the atmosphere is not accurately represented by an exponential decay model. Forster et al. approximated the $AGWP$ of CO_2 using Equation 6:

$$AGWP_{CO_2}(H) = A_{CO_2}\left\{a_o H + \sum_{i=1}^{3} a_i\alpha_i\left(1 - \exp\left(-\frac{H}{\alpha_i}\right)\right)\right\} \quad (6)$$

where A_{CO_2} is the RE of CO_2, $a_0 = 0.217$, $a_1 = 0.259$, $a_2 = 0.338$, $a_3 = 0.186$, $\alpha_1 = 172.9$ years, $\alpha_2 = 18.51$ years and $\alpha_3 = 1.186$ years. Based on Equation 6, the AGWP of CO_2 for a 20-year time horizon is 2.49 ×10^{-14} W·m^{-2}·yr·kg^{-1} and the AGWP of CO_2 for a 100-year time horizon is 9.17 ×10^{-14} W·m^{-2}·yr·kg^{-1}.[4]

If the net cooling power of a given RC structure is known, its AGWP can be approximated using Equation 7.[19]

$$AGWP_{RC_i}(H) = -\int_0^H \frac{P_{\text{net cooling},i}}{A_{RC_i}}\left(\frac{1}{A_{\text{tropopause}}}\right)dt \quad (7)$$

where RC_i denotes RC structure i, the cooling power for RC_i is $P_{\text{net cooling,i}}$, A_{RCi} is the area of RC_i projected onto the horizontal plane, and $A_{\text{tropopause}}$ is the area of the tropopause. The negative sign in Equation 7 indicates the $AGWP$ is negative when an RC structure has a positive net cooling effect. Moreover, the $(1/A_{\text{tropopause}})$ term in Equation 7 normalizes the AGWP of an RC structure to the area of the tropopause, which enables the GWP of the RC structure to be calculated in terms of CO_{2eq}. It follows that the GWP of an RC structure can be estimated using Equation 8:

$$GWP_{RC_i}(H) = \frac{AGWP_{RC_i}(H)}{AGWP_{CO_2}(H)} = \frac{-\int_0^H \frac{P_{\text{net cooling},i}}{A_{RC_i}}\left(\frac{1}{A_{\text{tropopause}}}\right)dt}{A_{CO_2}\left\{a_o H + \sum_{i=1}^{3} a_i\alpha_i\left(1 - \exp\left(-\frac{H}{\alpha_i}\right)\right)\right\}} \quad (8)$$

The GWP_{RCi} (H) values are determined in units of $kgCO_{2\text{-eq}}$·m^{-2} which, when multiplied by the area of the RC structure or panel, gives the desired units of $kgCO_{2\text{-eq}}$. The GWP_{RCi} values can be included when determining the total GWP of RC technologies in a LCA. Negative GWP_{RCi} values can be interpreted as credits for offsetting $CO_{2\text{-eq}}$ emissions, such as emissions released during the manufacturing of RC panels or while providing base cooling loads using conventional methods.

2.3. Determining the Global Warming Impact when Covering 1% of the Earth's Surface with RC Materials

The materials are evaluated based on their $\bar{R}_{\text{solar}}$, $\bar{\varepsilon}_{\text{LWIR}}$, net outgoing power, RF, and GWP over 20 and 100 years. It is assumed that 1% of the Earth's surface is covered by the materials listed in **Table 1** that reflect $\bar{R}_{\text{solar}}$ of the solar radiation of (163.3 + 22.9 W·m^{-2}) incident on the Earth's surface and emit $\bar{\varepsilon}_{LWIR}$/95% of the radiation emitted to space through the atmospheric window (which is 40.1 W·m^{-2} as shown in Figure 1). The remaining 99% of the Earth's surface remains the same and is assumed to have a radiative balance with outer space as depicted in Figure 1 (with RF = 0.6 W·m^{-2}).

Table 1. Classification of the materials examined and their $\bar{R}_{solar}$ and $\bar{\varepsilon}_{LWIR}$ values.

Structure		$\bar{R}_{solar}$ (%)	$\bar{\varepsilon}_{LWIR}$ (%)
ID	RC Structures in Literature		
I	Pirvaram et al.[29]	98.2	98.5
II	Wang et al.[30]	95	98
III	Li et al.[31]	96	78
	Common Construction Materials		
IV	White cement paste[36]	66	93
V	Road asphalt (ID A001)[37]	21	96
VI	Concrete (ID C002)[37]	21	92
VII	Grey cement (ID C005)[37]	41	95
	Common Roofing Materials		
VIII	Roofing shingle (ID L003)[37]	6	95
IX	Ceramic roofing tile (ID R010)[37]	19	95
X	PVC roofing material (ID V002)[37]	43	93
	Natural Surfaces		
XI	Forests[38]	15	97
XII	Oceans	10[39]	98[40]
	Reference Cases		
XIII	Perfect RC	100	100
XIV	Perfect reflector	100	0
XV	Blackbody	0	100

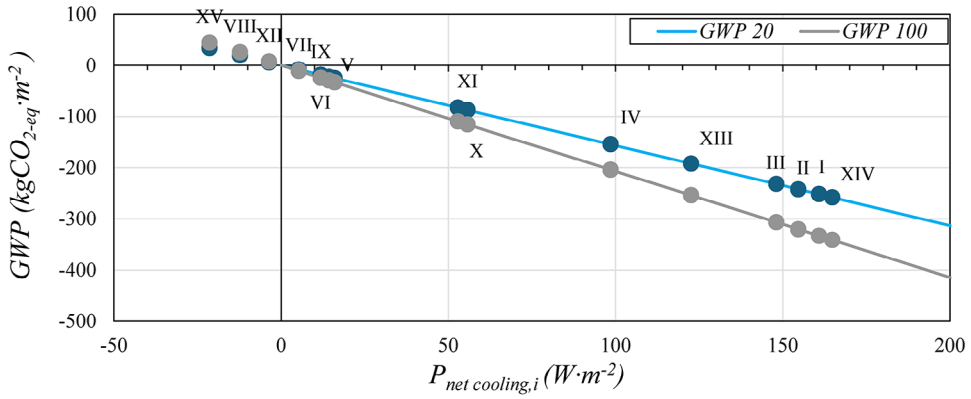

Figure 2. GWP as a function of cooling power for the materials listed in Table 1. (I = Pirvaram et al.,[29] II = Wang et al.,[30] III = Li et al.,[31] IV = White cement paste,[36] V = Road asphalt (ID A001),[37] VI = Concrete (ID C002),[37] VII = Grey cement (ID C005),[37] VIII = Roofing shingle (ID L003),[37] IX = Ceramic roofing tile (ID R010),[37] X = PVC roofing material (ID V002),[37] XI = Forests,[38] XII = Oceans,[39,40] XIII = Perfect RC, XIV = Perfect reflector, and XV = Blackbody).

The equation for calculating the *RF* at TOA when 1% of the Earth's surface is covered with material *i* (herein defined as $RF_{i(1\%)}$) is given as:

$$RF_{i(1\%)} = 1\% \times RF_i + 99\% \times RF_{\text{Earth}} \quad (9)$$

In this study, Equations 4 – 8 are utilized to calculate of $AGWP_{RCi}$ *(20)* $\text{W}\cdot\text{m}^{-2}\cdot\text{yr}\cdot\text{kg}^{-1}$, $AGWP_{RCi}$ *(100)* $\text{W}\cdot\text{m}^{-2}\cdot\text{yr}\cdot\text{kg}^{-1}$, GWP_{RCi} *(20)* $\text{W}\cdot\text{m}^{-2}\cdot\text{yr}\cdot\text{kg}^{-1}$, and GWP_{RCi} *(100)* $\text{W}\cdot\text{m}^{-2}\cdot\text{yr}\cdot\text{kg}^{-1}$, respectively.

3. Results and Discussion

3.1. Analysis of Net Cooling Power of RC Materials and their Associated Global Warming Potential

Figure 2 illustrates the GWP relative to the net cooling power, $P_{\text{net cooling}}$, of a surface, which provides valuable insights into the environmental benefits of using RC technologies to mitigate climate change impacts. The GWP_{RCi} values plotted in the figure represent the GWP per square meter of RC panel area over 20 years (GWP_{RCi} *(20)*) and 100 years (GWP_{RCi} *(100)*). The negative values of GWP_{RCi} indicate the cooling effect of the RC ma-

terials offset the warming due to CO_{2eq} emissions. Starting from zero at zero cooling power, the GWP_{RCi} values decrease linearly with increasing cooling power. For example, a RC structure of porous Poly(vinylidene fluoride-co-hexafluoropropylene) (PVDF-HFP) developed in reference[29] exhibits a solar reflectivity of $\bar{R}_{solar}$ = 98.2% and a long-wavelength infrared emissivity of $\bar{\varepsilon}_{LWIR}$ = 98.5%. Using the information obtained from Figure 1 and Equation 3, the $P_{net\ cooling}$, which is qual to $-RF_i$, is calculated to be 160.8 $W{\cdot}m^{-2}$ that leads to GWP_{RCi} *(20)* = −252 $kgCO_{2\text{-}eq}{\cdot}m^{-2}$ and GWP_{RCi} *(100)* = −333 $kgCO_{2\text{-}eq}{\cdot}m^{-2}$ using Equations 9 – 13. The negative values imply that 252 and 333 kg of CO_2 emissions are offset by the cooling achieved by 1 m^2 of a surface with this cooling power over 20-year and 100-year timeframes, respectively.

3.2. The Global Warming Impact when Covering 1% of the Earth's Surface with a RC Material

This section evaluates the impact of covering 1% of Earth's surface with the materials listed in Table 1 on the GWP. The optical properties of the materials outlined in Table 1 are used to calculate the net outgoing power, RF, and GWP over 20 and 100 years. The results are summarized in **Table 2** and displayed in **Figure 3**.

Among all surfaces considered. the hypothetical case of the black body has the highest GWP values of GWP(20) = 33.5 $kgCO_{2\text{-}eq}{\cdot}m^{-2}$ and GWP(100) = 44.3 $kgCO_{2\text{-}eq}{\cdot}m^{-2}$. Although a blackbody emits the maximum amount of radiation over the atmospheric window, it also absorbs 100% of the incident solar radiation, which results in substantial heating overall. Indeed, as shown in Figure 3, the RF at the TOA would increase from 0.6 to 0.81 if 1% of the Earth's surface were covered with a material that had the properties of a black body.

Notably, as shown in Table 2, only three types of surfaces would increase the GWP if they covered 1% of the Earth: Oceans, roofing shingles, and the hypothetical case of the blackbody. (Here, covering the Earth's surface with oceans refers to covering an area the size of 1% of Earth's surface that has an average solar reflectance of 12.3% and long-wave infrared emissivity of 95%). Ocean surfaces contribute to a slightly higher RF value than that for the average terrestrial surface. This raises concerns about RF values increasing as sea ice melts and exposes ocean waters. In contrast to water, which has an albedo of ≈10%,[39] ice has a significantly higher albedo of 49%.[41] This higher albedo allows ice to reflect a much greater portion of incoming solar radiation back into space compared to the darker ocean surfaces, despite both water and ice having nearly the same infrared emissivity of 98%[40] and 94.75%,[41] respectively. Applying these albedo and emissivity values of ice to Equation 3 results in a RF of −0.09 $W{\cdot}m^{-2}$, indicating the cooling effect that sea ice provides by reflecting solar radiation away from Earth's surface. However, as sea ice diminishes and darker ocean waters are exposed, this negative RF diminishes, contributing to further warming. In recent years, human-induced greenhouse gas emissions have driven numerous environmental issues, one of the most visible being the decline of sea ice. For example, satellite data from the GRACE and GRACE-FO missions, which have tracked changes in Greenland's ice sheet since May 2002,[42,43] show that Greenland has lost ≈4550 gigatons (4550 billion metric tons) of ice mass. This ice melt exposes darker ocean surfaces with much lower albedo,

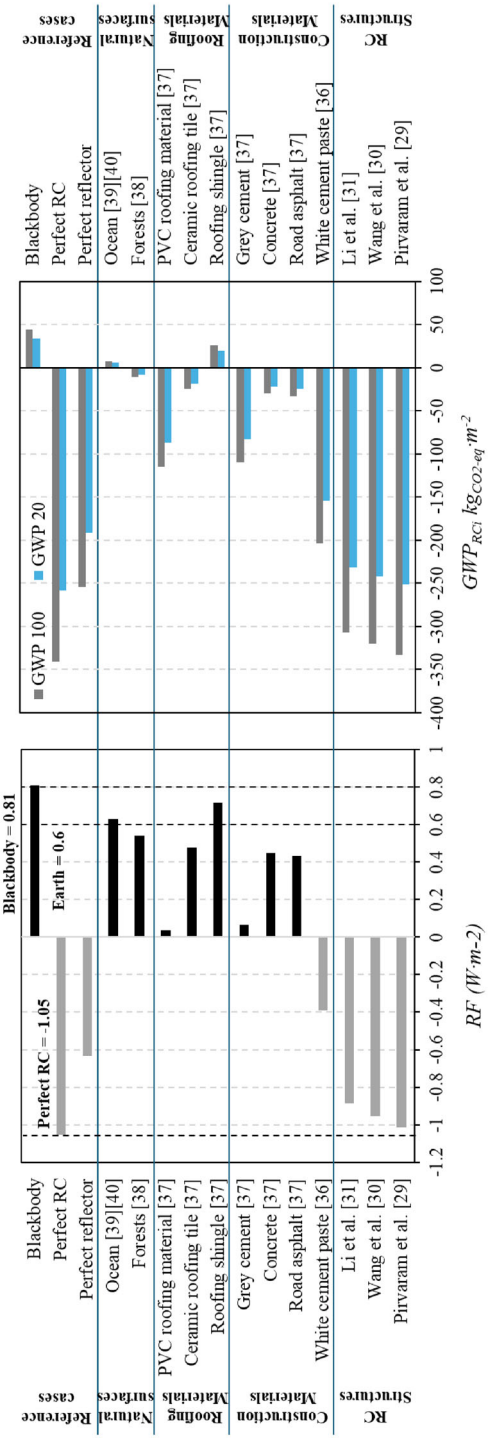

Figure 3. RF (left) and GWP (right) resulting from covering 1% of the Earth's surface with various materials. For the plot on the left black bars indicate positive RF values and grey bars represent negative RF values. The vertical black dashed lines labeled "Blackbody" and "Perfect RC" indicate the upper and lower limits on the RF attained when 1% of the Earth's surface is covered with a material. The vertical black line labeled 'Earth' indicates Earth's RF value of 0.6. For the plot on the right the grey and blue bars indicate the GWP for 100- and 20- year time frames, respectively.

Table 2. Net cooling power, GWP and RF associated with materials in Table 1.

Structure	$\bar{R}_{solar}$ (%), albedo	$\bar{\varepsilon}_{LWIR}$ (%)	$P_{net,\ Cooling}$ [$W \cdot m^{-2}$]	GWP_{RCi} (20) $kg_{CO2\text{-}eq} \cdot m^{-2}$	GWP_{RCi} (100) $kg_{CO2\text{-}eq} \cdot m^{-2}$	$RF_{1\%}$–TOA* [$W \cdot m^{-2}$]	$\Delta RF_{1\%}$ – TOA** [$W \cdot m^{-2}$]
Earth	12.3***	95	−0.6	9.40E-01	1.24E+00	0.6	0
RC Structures in Literature							
Pirvaram et al.[29]	98.2	98.5	160.8	−2.52E+02	−3.33E+02	−1.01	−1.61
Wang et al.[30]	95	98	154.6	−2.42E+02	−3.20E+02	−0.95	−1.55
Li et al.[31]	96	78	148	−2.32E+02	−3.07E+02	−0.89	−1.49
Common Construction Materials							
White cement paste[36]	66	93	98.5	−1.54E+02	−2.04E+02	−0.39	−0.99
Road asphalt (ID A001)[37]	21	96	16	−2.51E+01	−3.32E+01	0.43	−0.17
Concrete (ID C002)[37]	21	92	14.3	−2.25E+01	−2.97E+01	0.45	−0.15
Grey cement (ID C005)[37]	41	95	52	−8.28E+01	−1.09E+02	0.066	−0.534
Common Roofing Materials							
Roofing shingle (ID L003)[37]	6	95	−12.3	1.93E+01	2.55E+01	0.72	+0.12
Ceramic roofing tile (ID R010)[37]	19	95	11.9	−1.86E+01	−2.46E+01	0.48	−0.12
PVC roofing material (ID V002)[37]	43	93	55.7	−8.73E+01	−1.15E+02	0.037	−0.563
Natural Surfaces							
Forests[38]	15	97	5.3	−8.26E+00	−1.09E+01	0.54	−0.06
Oceans	10[39]	98[40]	−3.6	5.66E+00	7.49E+00	0.63	+0.03
Reference Cases							
Perfect RC	100	100	164.8	−2.58E+02	−3.41E+02	−1.05	−1.65
Perfect reflector	100	0	122.6	−1.92E+02	−2.54E+02	−0.63	−1.23
Blackbody	0	100	−21.4	3.35E+01	4.43E+01	0.81	+0.21

*RF at TOA when 1% of the Earth's surface is covered with the material.
**$\Delta\ RF_{1\%} = RF_{1\%} - RF_{Earth}$ where $RF_{Earth} = 0.6\ W \cdot m^{-2}$ at TOA.
***The average surface albedo of the Erath is 22.9/186.2 = 12.3%

leading to increased absorption of solar radiation. This, in turn, accelerates global warming by amplifying RF. The significant ice loss from Greenland has also contributed to a global sea level rise of ≈1.2 cm over the same period, marking a stark reminder of the growing impacts of climate change.[43]

For roofing shingles GWP(100) = 25.5 $kgCO_{2\text{-eq}}\cdot m^{-2}$, where as for the average terrestrial surface GWP(100) = 1.24 $kgCO_{2\text{-eq}}\cdot m^{-2}$. It follows that on average GWP(100) increases by 24.3 $kgCO_{2\text{-eq}}\cdot m^{-2}$ when roofing shingles are used. If 1% of the Earth were to be covered with roofing shingles the corresponding increase in GWP(100) would be ≈124 Gt $CO_{2\text{-eq}}$, which is more than thee times the amount of CO_2 emitted annually. Fortunately, as shown in Table 2, most construction and roofing materials have a positive net cooling effect and decrease GWP. Of the construction and roofing materials listed in Table 2 white cement paste is the best RC with $P_{net,cooling}$ = 98.5 $W\cdot m^{-2}$ and GWP(100) = −204 $kgCO_{2\text{-eq}}\cdot m^{-2}$. If 1% of the Earth's surface were to be replaced with white cement paste, the RF at the TOA would decrease from 0.6 to −0.39 $W\cdot m^{-2}$, implying the Earth would experience global cooling.

The upper limit on the achievable amount of cooling is set by the perfect RC material with $\bar{R}_{solar}$ = 100% and $\bar{\varepsilon}_{solar}$ = 100%. The net cooling power for this ideal material is 164.8 $W\cdot m^{-2}$ and if 1% of the Earth's surface were to be covered by a perfect RC, the RF would decrease from 0.6 to −1.05. Remarkably, engineered RC materials with net cooling abilities very close to that of the perfect RC have been fabricated. Pirvaram et al.,[25] Wang et al.,[26] and Li et al.[27] fabricated porous polymeric RC films exhibiting cooling values of $P_{net,cooling}$ = 160.8 W m^{-2}, $P_{net,cooling}$ = 154.6 W m^{-2}, and $P_{net,cooling}$ = 148 W m^{-2}, respectively. Covering 1% of the Earths surface with these materials would decrease the RF at the TOA to as low as −1.01 $W\cdot m^{-2}$.

To validate the results obtained in this study, the effects of albedo modifications on RF values is compared with that reported in existing studies. According to the research conducted by the MIT Concrete Sustainability Hub, increasing 1% of the Earth's average surface albedo can change the RF in a range of −1.3–−2.9 $W\cdot m^{-2}$, depending on the methodology and assumptions taken. [44] Akbari et al.[45] reported that a 1% increase in the urban areas' albedo could result in a reduction of the global RF to ≈−1.3 $W\cdot m^{-2}$. While Lenton and Vaughan[46] estimated that this urban albedo modification could achieve an RF of ≈−1.0 $W\cdot m^{-2}$. In a more recent study conducted by Hu et al.,[47] a potential RF reduction of −1.6 $W\cdot m^{-2}$ is reported. In the current study, covering 1% of the Earth's surface with a highly reflective RC material (albedo = 98.2%) while the remaining 99% retains an albedo of 12.3% effectively increases the global average albedo by ≈1%, resulting in a calculated RF of −1.61 W m^{-2} compared to the reference RF of 0.6 $W\cdot m^{-2}$ for Earth's surface. The value calculated herein falls within the reported range of RFs, which are between −1.3 and −2.9 W m^{-2}, confirming the consistency of the findings with established literature. The variations between studies can be attributed to differences in solar insolation, atmospheric transmittance, and surface characteristics considered in the models.

Reducing GWP by changing the albedo of surfaces and using RC materials over large areas have also been reported in the literature. Akbari et al.[45] investigated the effects of changing the albedo of surfaces of urban areas on a reduction in RF. They reported the emitted CO_2 offset for increasing roof albedo by 25% is equal to −64 $kgCO_{2\text{-eq}}\cdot m^{-2}$ of roof area. Similarly, for cool pavements with a proposed albedo difference of 0.15, the emitted CO_2 offset is equal to −38 $kgCO_{2\text{-eq}}\cdot m^{-2}$ of pavement area. Therefore, 16 m^2 of cool roof areas and 26 m^2 of cool paved areas are needed to offset 1 tonne of CO_2 emissions. Munday[48] suggested that if 5×10^6 km^2 in desert areas were to be covered with RC materials the terrestrial RF would be decreased by almost 1 $W\cdot m^{-2}$. In comparison, the GWP associated with the RC material fabricated by Pirvaram et al. is −333 $kgCO_{2\text{-eq}}\cdot m^{-2}$, and if 1% of Earth's surface (which is ≈5.1×10^6 km^2) were to be covered with this material the RF would decrease by 1.61 $W\cdot m^{-2}$ (from 0.6 to −1.01 $W\cdot m^{-2}$). Achieving such a low RF value shows the potential for using these RC materials for practical applications in reducing urban heat island effects and lowering energy consumption in buildings. Notably, it has been reported that the global urbanized land area is ≈3% of Earth's total land area.[49]

One limitation of this study is the use of surface albedo and emissivity results measured at normal incidence for the calculations. While these measurements provide useful insights, they do not account for the full angular dependence of radiative properties. It is important to note that these values may not fully capture the angular dependence of radiative properties. Solar reflectance (albedo) and long-wave IR emissivity can both vary significantly with the angle of incidence. As the angle between incident solar radiation and the normal to a surface increases, solar reflectance generally increases, leading to less absorption of solar energy. On the other hand, long-wave IR emissivity may also exhibit angular dependence, with emissivity often increasing as the angle of emission approaches the normal direction.[50] For a more detailed analysis, future work could consider hemispherical optical properties measured at different angles. This would provide a broader understanding of how surface reflectivity and emissivity vary, though the current results still offer valuable insights.

Another limitation is that the use of RC materials cannot be a permanent solution to greenhouse gas emissions. Similarly to SRM technologies, geoengineering via widespread RC can contribute to mitigating global warming and minimizing damage to ecosystems but will not address the underlying causes of global warming. Largescale RC will not be able to offset increases in global warming if greenhouse gas emissions continue to rise. Nevertheless, RC can play an important role in alleviating the effects of global warming while solutions that address the root causes of global warming are developed. To address global warming nations are transitioning to clean energy sources and developing carbon capture technologies.[51–53] However, almost half of the CO_2 that has already been emitted will stay in the atmosphere for centuries and will contribute to global warming over extended time periods.[54,55] RC technologies can play a vital role in "buying time" by offsetting RF caused by greenhouse gas emissions while permanent solutions for global warming are being developed and implemented.

Another important point to mention is that while RC materials offer significant benefits in reducing cooling energy demand and lowering CO_2 emissions, their effectiveness can be affected by seasonal variations. During cold seasons, the cooling effect of RC materials can lead to excessive cooling, which may increase heating demand and overall energy consumption. This seasonal trade-off is important to consider when evaluating the full en-

vironmental impact of RC materials, particularly when the effects of RCs on energy consumption are involved. To address this issue, Dynamic Thermal Regulation (DTR) strategies—such as thermochromic or switchable emissivity materials—can be employed. These strategies allow RC materials to adapt to varying climatic conditions by minimizing the risk of overcooling in colder environments. Through the integration of adaptive designs or hybrid systems, RC materials can be optimized for use across diverse environmental conditions, ensuring their practical application year-round. However, while DTR is crucial for optimizing energy savings, this study focuses primarily on the effects of RC materials on modifying Earth's radiative balance and contributing to a reduction in RF.

4. Conclusion

This study analyses RC materials in comparison with conventional construction and roofing materials and highlights their significant potential in mitigating global warming. The study reveals that RC materials with high solar reflectivity and long-wavelength infrared emissivity can notably reduce RF and GWP. Among the materials evaluated, those developed by Pirvaram et al.,[29] Wang et al.,[30] and Li et al.[31] exhibit notable cooling efficiencies and significant reductions in RF. The results suggest that covering 1% of the Earth's surface with high-performance RC materials could offset a considerable amount of anthropogenic CO_2 emissions, offering a practical approach to climate change mitigation. For example, the RC material developed by Pirvaram et al. demonstrates exceptional performance with a $\bar{R}_{solar}$ of 98.2% and a $\bar{\varepsilon}_{LWIR}$ of 98.5%. This material achieves a net cooling power of 160.8 $W{\cdot}m^{-2}$, leading to a GWP of −252 $kgCO_2{\text{-}eq{\cdot}m^{-2}}$ over 20 years and −333 $kgCO_2{\text{-}eq{\cdot}m^{-2}}$ over 100 years. Its RF value is −1.01 $W{\cdot}m^{-2}$ when covering 1% of the Earth's surface, indicating a substantial reduction in RF compared to conventional materials. These results are closely comparable with the perfect RC as the benchmark for performance (with $\bar{R}_{solar}$= $\bar{\varepsilon}_{LWIR}$= 100%), which shows a net outgoing power of 164.8 $W{\cdot}m^{-2}$ and achieves the highest reduction in RF ($\Delta RF = -1.05\ W{\cdot}m^{-2}$). On the other hand, roofing shingles (ID L003[37] with $\bar{R}_{solar}$ of 6% and $\bar{\varepsilon}_{LWIR}$ of 95%) shows the least favorable environmental impact among the materials analyzed. It sets a net cooling power of −12.3 $W{\cdot}m^{-2}$ and a GWP of 193 $kgCO_2{\text{-}eq{\cdot}m^{-2}}$ over 20 years and 255 $kgCO_2{\text{-}eq{\cdot}m^{-2}}$ over 100 years. The RF value for roofing shingle (ID L003)[37] is 0.72 $W{\cdot}m^{-2}$ when 1% of the Earth's surface is covered, indicating a positive contribution to RF and increasing global temperatures. The results emphasize that engineered RC materials offers superior cooling efficiency and potential for global warming mitigation, closely approaching the ideal perfect RC benchmark. In contrast, roofing shingles, along with other conventional materials like concrete and road asphalt, contributes positively to RF, highlighting their environmental drawbacks. The findings of this work underscore the importance of incorporating RC materials into sustainable building practices and climate mitigation strategies.

Acknowledgements

This research was supported by the Natural Sciences and Engineering Research Council of Canada (RGPIN-2024-06245 and RGPIN-2022-04566).

Conflict of Interest

The authors declare no conflict of interest.

Data Availability Statement

The data that support the findings of this study are available from the corresponding author upon reasonable request.

Keywords

geoengineering, global warming, life-cycle assessment, radiative cooling, radiative forcing

Received: November 28, 2024
Revised: March 3, 2025
Published online: March 27, 2025

[1] M. Allen, M. Babiker, Y. Chen, H. de Coninck, S. Connors, R. van Diemen, K. Zickfeld, 2018. Global Warming of 1.5°C:Special Report on the Impacts of Global Warming. Geneva: Intergovernmental Panel on Climate Change (IPCC).
[2] K. P. Shine, *Space Sci. Rev.* **2000**, *94*, 363.
[3] Hodnebrog, M. E., J. S. Fuglestvedt, G. Marston, G. Myhre, C. J. Nielsen, K. P. Shine, T. J. Wallington, *Rev. Geophys.* **2013**, *51*, 300.
[4] P. Forster, V. Ramaswamy, P. Artaxo, T. Berntsen, R. Betts, D. W. Fahey, J. Haywood, J. Lean, D. C. Lowe, G. Myhre, J. Nganga, R. Prinn, G. Raga, M. Schulz, R. van Dorland, *in Climate Change 2007: The Physical Science Basis. Contribution of Working Group I to the Fourth Assessment Report of the Intergovernmental Panel on Climate Change*, Eds. S. Solomon, D. Qin, M. Manning, Z. Chen, M. Marquis, K. B. Averyt, M. Tignor, H. L. Miller, Cambridge University Press, Cambridge, United Kingdom and New York, NY, USA, **2007**
[5] H. E. Armstrong, *Nature* **1931**, *127*, 600.
[6] S. Fawzy, A. I. Osman, J. Doran, D. W. Rooney, *Environ. Chem. Lett.* **2020**, *18*, 2069.
[7] C. E. Wieners, B. P. Hofbauer, I. E. de Vries, M. Honegger, D. Visioni, H. W. J. Russchenberg, T. Felgenhauer, *Oxford Open Clim. Chang.* **2023**, *3*, 4.
[8] H. K. Jeswani, D. M. Saharudin, A. Azapagic, *Sustain. Prod. Consum.* **2022**, *33*, 608.
[9] S. Cobo, V. Negri, A. Valente, D. M. Reiner, L. Hamelin, N. M. Dowell, G. Guillén-Gosálbez, *Environ. Res. Lett.* **2023**, *18*, 023001.
[10] International Energy Agency (IEA), **2018**, 92.
[11] B. Ko, D. Lee, T. Badloe, J. Rho, *Energies* **2019**, *12*, 1.
[12] L. Pérez-Lombard, J. Ortiz, C. Pout, *Energy Build.* **2008**, *40*, 394.
[13] V. Costanzo, G. Evola, L. Marletta, *Adv. Build. Energy Res.* **2013**, *7*, 155.
[14] H. Fang, D. Zhao, J. Yuan, A. Aili, X. Yin, R. Yang, G. Tan, *Appl. Energy* **2019**, *248*, 589.
[15] B. Zhao, M. Hu, X. Ao, G. Pei, *Appl. Energy* **2017**, *205*, 626.
[16] J. Chen, L. Lu, Q. Gong, W. Y. Lau, K. H. Cheung, *Energy Convers. Manag.* **2021**, *245*, 114621.
[17] T. L. Bergman, *Sol. Energy* **2018**, *174*, 16.
[18] A. Castaldo, G. Vitiello, E. Gambale, M. Lanchi, M. Ferrara, M. Zinzi, *Energies* **2020**, *13*, 1.
[19] A. Pirvaram, N. Talebzadeh, S. N. Leung, P. G. O'Brien, *Renew. Sustain. Energy Rev.* **2022**, *162*, 112415.
[20] A. Kafaei, A. Pirvaram, K. Karbasishargh, F. Massah, S. N. Leung, E. Lakzian, P. G. O'Brien, *Energy Technol.* **2024**, *12*, 1.
[21] L. Li, G. Liu, Q. Zhang, H. Zhao, R. Shi, C. Wang, Z. Li, B. Zhou, Y. Zhang, *ACS Appl. Mater. Interfaces* **2024**, *16*, 6504.

[22] J. Song, Q. Shen, H. Shao, X. Deng, *Adv. Sci.* **2024**, *11*, 2305664.
[23] S. So, J. Yun, B. Ko, D. Lee, M. Kim, J. Noh, C. Park, J. Park, J. Rho, *Adv. Sci.* **2024**, *11*, 1.
[24] H. Di Wang, C. H. Xue, C. Q. Ma, X. X. Jin, M. C. Huang, Y. G. Wu, S. Q. Lv, A. J. Chang, J. Li, X. J. Guo, *ACS Sustainable Chem. Eng.* **2024**, *12*, 1681.
[25] S. Liu, F. Zhang, X. Chen, H. Yan, W. Chen, M. Chen, *J. Energy Chem.* **2024**, *90*, 176.
[26] A. Pirvaram, T. Cooper, S. N. Leung, P. G. O'Brien, *Energy Convers. Manag.* **2024**, *304*, 118180.
[27] P.-C. Chiu, A. Pirvaram, T. Cooper, S. N. Leung, P. G. O'Brien, work in preparation, **2025**.
[28] N. Guo, C. Shi, N. Warren, E. A. Sprague-Klein, B. W. Sheldon, H. Yan, M. Chen, *Adv. Energy Mater.* **2024**, *2401776*, 1.
[29] A. Pirvaram, P. G. O'Brien, S. N. Leung, "Fabrication and Optimization of Highly Solar Reflective and Long-Wavelength Infrared (LWIR) Emissive Porous Polymers for Passive Daytime Radiative Cooling," in Advanced Photonics Congress 2024, Technical Digest Series (Optica Publishing Group, 2024), paper JM3D.3.
[30] T. Wang, Y. Wu, L. Shi, X. Hu, M. Chen, L. Wu, *Nat. Commun.* **2021**, *12*, 1.
[31] D. Li, X. Liu, W. Li, Z. Lin, B. Zhu, Z. Li, J. Li, B. Li, S. Fan, J. Xie, J. Zhu, *Nat. Nanotechnol.* **2021**, *16*, 153.
[32] N. G. Loeb, B. A. Wielicki, D. R. Doelling, G. L. Smith, D. F. Keyes, S. Kato, N. Manalo-Smith, T. Wong, *J. Clim.* **2009**, *22*, 748.
[33] K. E. Trenberth, J. T. Fasullo, J. Kiehl, *Bull. Am. Meteorol. Soc.* **2009**, *90*, 311.
[34] G. C. Johnson, J. M. Lyman, N. G. Loeb, *Nat. Clim. Chang.* **2016**, *6*, 639.
[35] P. Balcombe, J. F. Speirs, N. P. Brandon, A. D. Hawkes, *Environ. Sci. Process. Impacts* **2018**, *20*, 1323.
[36] J. S. Dolado, G. Goracci, S. Arrese-Igor, A. Ayuela, A. Torres, I. Liberal, M. Beruete, J. J. Gaitero, M. Cagnoni, F. Cappelluti, *ACS Appl. Opt. Mater.* **2023**, *2*, 1000.
[37] S. Kotthaus, T. E. L. Smith, M. J. Wooster, C. S. B. Grimmond, *ISPRS J. Photogramm. Remote Sens.* **2014**, *94*, 194.
[38] H. C. Ward, S. Kotthaus, L. Järvi, C. S. B. Grimmond, *Urban Clim.* **2016**, *18*, 1.
[39] R. Seitz, *Clim. Change* **2011**, *105*, 365.
[40] M. Konda, N. Imasato, K. Nishi, T. Toda, *J. Oceanogr.* **1994**, *50*, 17.
[41] E. Schmidt, Forschung: Zeitschrift für Technische Mechanik und Thermodynamik, **1934**, *5*, 1.
[42] E. L. Emry, D. A. Wiens, D. Garcia-Castellanos, *AGU J. Geophys. Res. Solid Earth* **2014**, *119*, 3076.
[43] D. N. Wiese, D.-N. Yuan, C. Boening, F. W. Landerer, M. M. Watkins. 2018. JPL GRACE Mascon Ocean, Ice, and Hydrology Equivalent Water Height Release 06 Coastal Resolution Improvement (CRI) Filtered Version 1.0. Ver. 1.0. PO.DAAC, CA, USA. Dataset accessed [2024-10-16] at http://dx.doi.org/10.5067/TEMSC-3MJC6
[44] .X, Xu, J. Gregory, R. Kirchain, *MIT CSHub* **2015**, *12*, 1.
[45] H. Akbari, S. Menon, A. Rosenfeld, *Clim. Change* **2009**, *94*, 275.
[46] T. M. Lenton, N. E. Vaughan, *Atmos. Chem. Phys.* **2009**, *9*, 5539.
[47] Y. Hu, G. Jia, C. Pohl, X. Zhang, J. van Genderen, *Theor. Appl. Climatol.* **2016**, *123*, 711.
[48] J. N. Munday, *Joule* **2019**, *3*, 2057.
[49] Z. Liu, C. He, Y. Zhou, J. Wu, *Landsc. Ecol.* **2014**, *29*, 763.
[50] Á. Andueza, C. Pinto, D. Navajas, J. Sevilla, *Opt. Mater.* **2021**, *121*, 111511.
[51] T. Sahu, K. K. Ghuman, P. G. O'Brien, *Prog. Sustain. Dev. Sustain. Eng. Pract*, Elsevier, Amsterdam, Netherlands **2023**, 205.
[52] K. S. Lackner, S. Brennan, J. M. Matter, A. H. A. Park, A. Wright, B. Van Der Zwaan, *Proc. Natl. Acad. Sci. USA* **2012**, *109*, 13156.
[53] A. Dubey, A. Arora, *J. Clean. Prod.* **2022**, *373*, 133932.
[54] D. Archer, *How Humans Are Changing the Next 100,000 Years of Earth's Climate*, Princeton University Press, Princeton **2016**.
[55] H. D. Matthews, *Tellus, Ser. B Chem. Phys. Meteorol.* **2006**, *58*, 591.